Simultaneous analyses of elastic scattering and fusion cross sections for the $^{32}S+^{58,64}Ni$ systems at energies near the Coulomb barrier

T. Udagawa and T. Tamura*
Department of Physics, University of Texas, Austin, Texas 78712

B. T. Kim
Department of Physics, Sung Kyun Kwan University, Suwon 440-746, Korea
(Received 12 September 1988)

Based on the optical model, simultaneous χ^2 analyses are performed on elastic scattering and fusion cross sections measured for the $^{32}S+^{58,64}Ni$ systems at several energies around the Coulomb barrier. We take the imaginary part of the optical potential used to consist of a surface-type direct and a volume-type fusion terms, W_D and W_F, respectively, the latter of which accounts for fusion. It is shown that such analyses can determine W_F and W_D fairly unambiguously, and that the potentials thus determined explain all of the characteristic features observed in the elastic scattering, fusion, and direct reaction cross sections. It is also shown that the potential satisfies the dispersion relation at the strong absorption radius.

Data have recently been accumulated for cross sections of elastic scattering (σ_{EL}),[1] fusion (σ_F),[2] and total quasi-elastic transfer reactions[3] (σ_{TR}) for the $^{32}S+^{58,64}Ni$ systems at several energies around the Coulomb barrier. The authors of Ref. 3 estimated the total inelastic scattering cross sections, and added them to the measured σ_{TR} to obtain the total direct reaction (DR) cross section σ_D. At the energies concerned the cross section for inelastic scattering is dominated by scattering to the first excited 2^+ and 3^- states. Since the cross sections to reach these states can be estimated fairly reliably, σ_D thus obtained may be expected to represent well the experimental DR cross section. Therefore for the above two systems data are now available for three different experimental cross sections σ_{EL}^{exp}, σ_F^{exp}, and σ_D^{exp}.

The data thus accumulated showed many interesting features such as the sub-barrier enhancement[4] of σ_F^{exp}, correlation[5] of the enhancement of σ_F^{exp} with the magnitude of σ_D^{exp}, and also the so-called threshold anomaly[6,7] (i.e., a rather striking energy dependence of the optical potentials deduced from σ_{EL}^{exp}). The enhancement of the sub-barrier σ_F has been well known for some time, while the latter two features were revealed fairly recently,[5-7] becoming subjects of current interest.

The final goal of nuclear reaction theory is to describe all the different type of reactions on a single footing. This has not been achieved in the past; particularly, fusion has been described based on the barrier penetration model (BPM),[4] which is somewhat different from DR theory (including the optical model) used for describing elastic scattering and direct reactions.

In order to improve the situation, we proposed[8] some time ago an approach which describes σ_F within the framework of the DR theory (optical model). The basic idea is to divide the imaginary part of the optical potential W into two portions, the fusion and DR portions, W_F and W_D, respectively, and to obtain σ_F as the portion to W_F of the total reaction cross section σ_R.

In the present study, we apply the method to analyze data taken for the $^{32}S+^{58,64}Ni$ systems[1-3] previously mentioned. More specifically, we carry out simultaneous χ^2 analyses[9] of σ_{EL}^{exp} and σ_F^{exp}. (We excluded in this study σ_D^{exp}, since σ_D^{exp} is not completely experimental. However, we shall compare the calculated σ_D with σ_D^{exp}.) The primary aim of this study is to demonstrate that such χ^2 analyses enable us to determine W_F and W_D, along with the real potential V_N, fairly unambiguously except at very low energies, and that the potentials thus determined explain all of the characteristic features of the observed data previously discussed.

The fusion and DR cross section formulas that we use in the present study are given in terms of W_F and W_D as[8]

$$\sigma_F=\frac{2}{v\hbar}\langle\chi^{(+)}|W_F(r)|\chi^{(+)}\rangle\ , \tag{1}$$

$$\sigma_D=\frac{2}{v\hbar}\langle\chi^{(+)}|W_D(r)|\chi^{(+)}\rangle\ . \tag{2}$$

Here v is the incident velocity and $\chi^{(+)}$ is the distorted wave calculated by using the *full* optical potential U,

$$U(r)=-V_N(r)+V_C(r)-i[W_F(r)+W_D(r)]\ . \tag{3}$$

In (3), V_N and V_C are the real nuclear and Coulomb potentials, respectively. The latter potential V_C is that of a uniformly charged sphere with radius parameter $r_C=1.25$ fm. Further, we assume for V_N, W_F, and W_D the following forms:

$$V(r)=\frac{V_R}{1+\exp(X_R)}\ , \tag{4}$$

$$W_F(r)=\frac{W_F}{1+\exp(X_F)}\ , \tag{5}$$

$$W_D(r)=4W_D\frac{\exp(X_D)}{[1+\exp(X_D)]^2}\ . \tag{6}$$

$X_i(i=R,\ F,\ \text{or}\ D)$ in Eqs. (4)–(6) is defined as $X_i=(r-R_i)/a_i$ with $R_i=r_i(A_1^{1/3}+A_2^{1/3})$.

As seen, V_N and W_F have the usual Woods-Saxon form, while W_D has a rather unusual, surface derivative form. Use of such a W_D was motivated by a recent study by Satchler *et al.*[10] They performed large scale coupled-channel (CC) calculations, and deduced an effective W_D by projecting the CC problem onto the one-dimensional optical-model problem. The best W_D thus deduced turned out to be a surface derivative type potential such as given by (6).

There are in all nine parameters involved in the optical potential U given by (3) with (4)–(6). Because of the well-known ambiguity of the potential parameters, it is impossible to determine the values of all these parameters from the χ^2 analysis. Two successive search procedures were thus used to determine the values. In the first procedure, we freely varied only three parameters, V_R, W_D and r_F. These three parameters are chosen as representative of the three parts of U. The other parameters were fixed to be $r_R=1.247$ fm, $a_R=0.53$ fm, $W_F=10$ MeV, $a_F=0.25$ fm, $r_D=1.50$ fm, and $a_D=0.79$ fm. Values for the real potential (a_R and r_R) are taken from Ref. 1, while those for the imaginary potentials (W_F, a_F, r_D, and a_D)

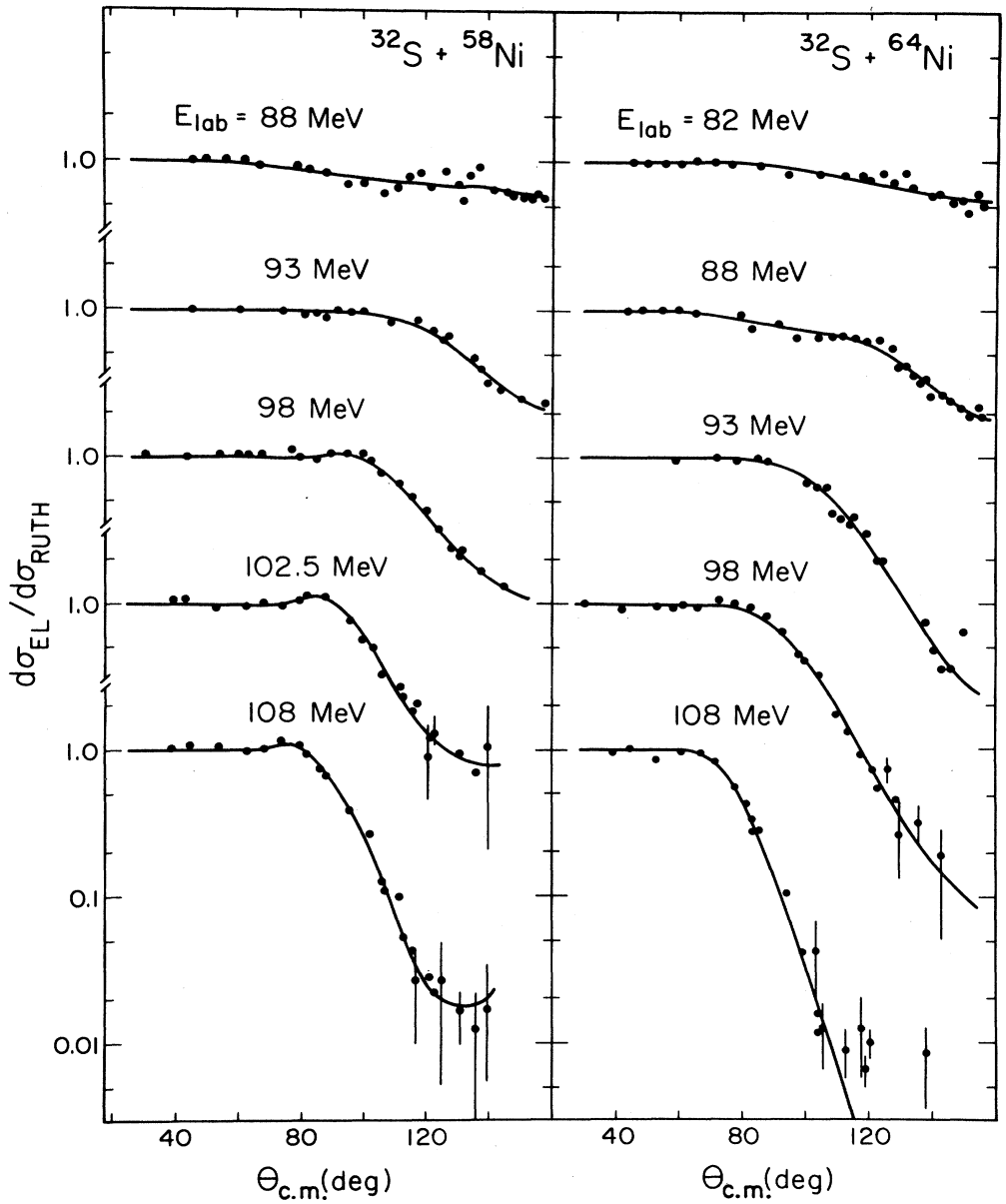

FIG. 1. Comparison of calculated and experimental elastic scattering cross sections (ratios to Rutherford) for the $^{32}S+^{58,64}Ni$ systems. The experimental cross sections are taken from Ref. 1.

are from Ref. 10. Note that the values of W_F, a_F, r_D, and a_D are those determined from the CC study[10] as previously remarked.

Even in this search with three free parameters, we were able to fit the observed elastic scattering and fusion cross sections fairly well. The best fit values of r_F turned out to be in a narrow range between 1.30 and 1.42 fm. (The average values with the mean deviations are 1.35 ± 0.04 and 1.39 ± 0.02 fm for the $^{32}S+^{58}Ni$ and $^{32}S+^{64}Ni$ systems, respectively.) The values thus determined are quite large, much larger than the critical distance r_{cr} assumed in the BPM,[4] and also much larger than $r_F=r_I=1.0$ fm used in all the CC calculations[10–14] made recently, but is very close to $r_F\simeq1.43$ fm determined from the analysis of the fusion data.[8] We note that the r_F values are determined rather unambiguously. This was confirmed by carrying out χ^2 analyses including W_F as an additional free parameter (four parameter fit). Even if W_F is added as a free parameter, the r_F values determined stayed essentially the same as those determined without it.

We also note that a large r_F value is required not only by $\sigma_F^{\rm exp}$, but also by $\sigma_{\rm EL}^{\rm exp}$. This was confirmed by performing χ^2 analyses without including $\sigma_F^{\rm exp}$, i.e., by considering only $\sigma_{\rm EL}^{\rm exp}$. The averages of the r_F values obtained from such an analysis turned out to be 1.40 and 1.39 fm for the $^{32}S+^{58}Ni$ and $^{32}S+^{64}Ni$ systems, respectively. These values agree very well with those obtained above from the analysis that includes σ_F. This shows that the elastic scattering data carries information on the r_F value, and thus underscores the importance of including $\sigma_{\rm EL}^{\rm exp}$ in a determination of r_F.

As previously remarked, the three parameter fit to the data was fairly good. It was, however, not completely free from trouble. In fact we noticed two unsatisfactory features. Firstly, the fit to the data at lower energies is somewhat worse than the fit obtained at higher energies, and secondly, the fit for the shoulder region of the angular distributions, particularly for the $^{32}S+^{58}Ni$ system at higher energies, was not completely satisfactory. After a few attempts, however, we noticed that the fit at low energies could be improved by increasing the r_D value, and the trouble at the shoulder could be removed by reducing a_F and slightly increasing r_F. (A similar conclusion was also reached in a more systematic parameter search made in Ref. 9.) The second procedure was thus used to improve the fit, where we fixed the values of a_F to be somewhere in between 0.1 and 0.35 fm and r_F to be 1.41 fm. The value of r_D was also fixed to be 1.518 and 1.50 fm for the $^{32}S+^{58}Ni$ and $^{32}S+^{64}Ni$ systems, respectively, except for the cases with the lowest energy, where the value was chosen to be $r_D=1.77$ fm. Further, the V_R values are fixed to be the same as those determined from the first procedure. We then searched the values of a_R, W_F, W_D, and a_D.

Figures 1 and 2 show the fit obtained in this way. The values of the parameters used in the calculation, and also fixed from the analysis, are all summarized in Table I. The calculated and experimental σ_D are also included there. As seen in Figs. 1 and 2, and also Table I, the resemblance of the calculated cross sections to the data is very satisfactory. As previously remarked, the experimental $\sigma_{\rm EL}$ for the $^{32}S+^{64}Ni$ system tends to fall off much faster than the $^{32}S+^{58}Ni$ system does, and also the enhancement of σ_F for the $^{32}S+^{64}Ni$ system is much more remarkable than that for the $^{32}S+^{58}Ni$ system. These features are all reproduced well in the calculation. The good fit to the σ_D data implies that the observed correlation[2] is also explained by the calculation.

Concerning the value of σ_D, it is important to remark that the present calculation predicted, at $E_{\rm lab}=88$ MeV, anomalously large σ_D values for both the $^{32}S+^{58}Ni$ and $^{32}S+^{64}Ni$ systems. Such large values originate from the fact that at this energy $\sigma_{\rm EL}^{\rm exp}$ (in units of the Rutherford cross section) starts to deviate from unity at an anomalously small angle of $\theta\simeq65°$. In fact, this angle is much smaller than similar deviation angles at higher energies, even smaller than that at the highest energy for the $^{32}S+^{58}Ni$ case. In order to explain this anomalous behavior of $\sigma_{\rm EL}^{\rm exp}$, the present χ^2 analysis required that the diffuseness parameter a_D takes an extremely large value, as seen in Table I. This in turn made the resultant σ_D be very large. At this moment, the physical reason of this anomaly is not known. However, we may ascribe it to an effect of some direct reactions, since the anomaly at small angles should be related to reactions taking place at a large distance. Unfortunately, data for the direct reactions are not available at present. In view of what was discussed above, it is important that measurements of the direct reaction cross sections be done.

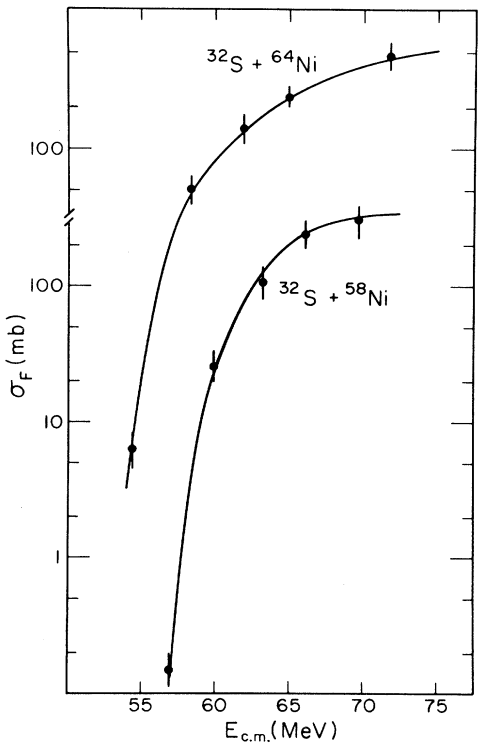

FIG. 2. Comparison of calculated and experimental fusion cross sections for the $^{32}S+^{58,64}Ni$ systems. The experimental cross sections are taken from Ref. 2.

TABLE I. The values of the optical potential used in the calculations of cross sections shown in Figs. 1 and 2 along with the values of σ_D, $\sigma_D^{\exp}$ and χ^2. The parameters fixed during the χ^2 search are underlined. The values of $\sigma_D^{\exp}$ are taken from Ref. 3.

SYSTEM	$^{32}S+^{58}Ni$					$^{32}S+^{64}Ni$				
E_{lab} (MeV)	88	93	98	102	108	82	88	93	98	108
V (MeV)	56.3	63.2	53.7	39.3	37.9	91.8	65.1	64.0	55.5	45.1
r_0 (fm)	1.247	1.247	1.247	1.247	1.247	1.247	1.247	1.247	1.247	1.247
a_0 (fm)	0.583	0.545	0.556	0.590	0.523	0.559	0.580	0.483	0.437	0.456
W_D (MeV)	0.102	0.441	0.423	0.540	0.950	0.252	0.235	0.816	0.929	0.831
r_D (fm)	1.77	1.518	1.518	1.518	1.518	1.770	1.500	1.500	1.500	1.500
a_D (fm)	1.46	0.510	0.382	0.355	0.237	0.381	1.370	0.499	0.491	0.486
W_F (MeV)	0.009	10.15	17.23	27.88	10.21	5.04	10.7	6.84	13.32	6.72
r_F (fm)	1.41	1.41	1.41	1.41	1.41	1.41	1.41	1.41	1.41	1.41
a_F (fm)	0.10	0.10	0.10	0.18	0.18	0.10	0.20	0.30	0.30	.35
σ_D	474	190	185	218	292	225	501	337	404	492
$\sigma_D^{\exp}$		152	205		306			286	335	498
χ^2	1.44	0.60	0.21	0.75	1.48	1.13	0.62	2.57	1.42	2.67

Figures 3(a) and (b) show the values of the resultant V and W $(=W_F+W_D)$ at $r=11.2$ and 11.4 fm (approximately corresponding to the strong absorption radii R_A) for the $^{32}S+^{58}Ni$ and $^{32}S+^{64}Ni$ systems, respectively. Such values are presented as functions of the incident center of mass energy $E_{c.m.}$ and are represented by the solid circles. We note that the values shown in Fig. 3 agree fairly well with those of the potentials determined in Ref. 1 from the analyses of $\sigma_{EL}^{\exp}$. The solid lines drawn for W represent values predicted from the following function:[15,16]

$$W(E_{c.m.})=W_0/[1+\exp(E_0-E_{c.m.})/a] , \quad (7)$$

with $W_0=0.36$ (0.72) MeV, $E_0=57.5$ (59.0) MeV, and $a=1.2$ (0.8) MeV for the ^{58}Ni (^{64}Ni) case. As seen, the W given by Eq. (7) reproduces the empirical W values fairly well. The broken lines drawn for W are two or three segments of straight lines, another parametrization of W. The lines drawn for V will be discussed later.

A remarkable feature of W is that it tends to increase sharply as $E_{c.m.}$ approaches the Coulomb barrier

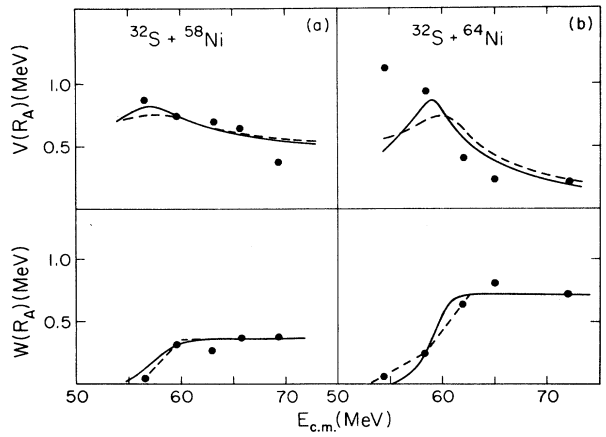

FIG. 3. The values of the real (V) and imaginary (W) potentials at the strong absorption radius as functions of $E_{c.m.}$. The solid and dashed lines drawn for V were obtained from the dispersion relation, using the W shown by the solid and dashed lines, respectively.

$E_{c.m.}\simeq 60$ MeV (threshold anomaly[5,6]). Further, the threshold anomaly appears more remarkably in the $^{32}S+^{64}Ni$ system than in the $^{32}S+^{58}Ni$ system, reflecting the fact that W for the $^{32}S+^{64}Ni$ system is larger by about a factor of 2 than that for the $^{32}S+^{58}Ni$ system. It may be worthwhile to note here that W for the $^{32}S+^{58}Ni$ system is dominated by W_D. This is not the case for the $^{32}S+^{64}Ni$ system, however, and in fact for this case approximately 25% of W originates from W_F. The rest comes from W_D. Nevertheless, the resultant W_D for the $^{32}S+^{64}Ni$ system is still larger by about a factor 1.5 than W $(\simeq W_D)$ of the $^{32}S+^{58}Ni$ system. These two features explain why both σ_F and σ_D for the $^{32}S+^{64}Ni$ system are larger than those for the $^{32}S+^{58}Ni$ system.

We now turn to the values of V shown in Fig. 3. As seen, the values of V also show the threshold anomaly,[6,7] i.e., tend to increase as $E_{c.m.}$ approaches the Coulomb barrier. Note that here the threshold anomaly again appears more remarkably in the $^{32}S+^{64}Ni$ system than in the $^{32}S+^{58}Ni$ system. We may now show that the empirically determined V and W approximately satisfy the following dispersion relation:[16,17]

$$V(E)=V(E_s)+\frac{E-E_s}{\pi}P\int_0^{\infty}dE'\frac{W(E')}{(E'-E_s)(E'-E)} . \quad (8)$$

In (8), P denotes the principal value and $V(E_s)$ is the value of the potential at $E=E_s$.

The solid and broken lines drawn for V in Fig. 3 are the V values predicted from the above dispersion relation using the W values shown in Fig. 3 by the solid and broken lines, respectively. As seen, the two sets of W qualitatively predict the same V values. Also, the V values thus predicted fit fairly well the empirical values, except the value for the $^{32}S+^{64}Ni$ system at the lowest energy $E_{c.m.}=54$ MeV. At this energy, the predicted V value is much smaller than the empirical value. This discrepancy, however, should not be taken seriously, since the V value at such a low energy is not determined very well. In fact, the use of the real potential, whose value at $r=R_A$ is 0.44 MeV, instead of 1.12 MeV as shown in

Fig. 3, gives a fairly good fit to the data. The change in the χ^2 value by the above change of the V value is only 25%. We may thus conclude that the empirical V and W values satisfy the dispersion relation.

Summarizing, we have performed simultaneous analyses of elastic scattering and fusion data within the framework of the direct reaction theory (optical model). We have demonstrated that in this way, we are able to extract the fusion and direct reaction parts of W, W_F, and W_D, separately, along with the real potential V_N. We have demonstrated that the potentials thus extracted show many interesting features, which explain all the characteristic features of the observed σ_F, σ_D, and σ_{EL}. We have also demonstrated that V and W thus extracted satisfy a dispersion relation[16,17] at the strong absorption radius.

We are grateful to Professor W. R. Coker and Dr. S. A. Stotts for their careful reading of the manuscript. This work was supported in part by the U.S. Department of Energy and by the Ministry of Education, Korea, through the Basic Science Research Institute Program, 1988.

---

*Deceased.

[1]A. M. Stefanini *et al.*, Phys. Rev. Lett. **59**, 2852 (1987).

[2]A. M. Stefanini *et al.*, Nucl. Phys. **A456**, 509 (1986).

[3]A. M. Stefanini *et al.*, Phys. Lett. B **185**, 15 (1987).

[4]See, for instance, a review article by J. R. Birkelund, and J. R. Huizenga, Annu. Rev. Nucl. Part. Sci. **33**, 265 (1983).

[5]K. E. Rehm, F. L. H. Wolfs, A. M. van den Berg, and W. Henning, Phys. Rev. Lett. **55**, 280 (1985).

[6]J. S. Lilley, B. R. Fulton, M. A. Nagarajan, I. J. Thompson, and D. W. Banes, Phys. Lett. **151B**, 181 (1985).

[7]B. R. Fulton, D. W. Banes, J. S. Lilley, M. A. Nagarajan, and I. J. Thompson, Phys. Lett. **162B**, 55 (1985).

[8]T. Udagawa, B. T. Kim, and T. Tamura, Phys. Rev. C **32**, 124 (1985).

[9]A similar simultaneous χ^2 analysis was made recently in somewhat different context for data of the $^{16}O+^{208}Pb$ system; see S. W. Hong, T. Udagawa, and T. Tamura, Nucl. Phys. **A491**, 492 (1989).

[10]G. R. Satchler, M. A. Nagarajan, J. S. Lilley, and I. J. Thompson, Ann. Phys. (N.Y.) **178**, 110 (1987).

[11]C. H. Dasso, S. Landowne, and A. Winther, Nucl. Phys. **A405**, 381 (1983).

[12]M. J. Rhoades-Brown and M. Prakash, Phys. Rev. Lett. **53**, 333 (1984); M. J. Rhoades-Brown and P. Braun-Munzinger, Phys. Lett. **136B**, 19 (1984).

[13]S. Landowne and S. C. Pieper, Phys. Rev. C **29**, 1352 (1984); S. C. Pieper, M. J. Rhoades-Brown, and S. Landowne, Phys. Lett. **162B**, 43 (1985).

[14]I. J. Thompson, M. A. Nagarajan, J. S. Lilley, and B. R. Fulton, Phys. Lett. **157B**, 250 (1985).

[15]C. Mahaux, H. Ngo, and G. R. Satchler, Nucl. Phys. **A449** 354 (1986); **A456**, 134 (1986).

[16]B. T. Kim, H. C. Kim, and K. E. Perk, Phys. Rev. C **37**, 998 (1988).

[17]C. Mahuax and H. Ngo, Nucl. Phys. **A378**, 205 (1982); M. A. Nagarajan, C. C. Mahaux, and G. R. Satchler, Phys. Rev. Lett. **54**, 1136 (1985).